Taking the Guesswork out of Antenna Ground and Spillover Noise

Peter W East

Abstract

Radio telescope antennas intercept ground radiation in their side- and back-lobes or via reflector spillover with a consequent loss in system sensitivity. Rough estimations, given average side- and back-lobe levels, are generally used [1,2]. With standard antenna co- and cross-polar E and H patterns it is possible to integrate over offending regions to fully determine ground effects on the system noise temperature [3,4]. This note describes a simple spreadsheet approach for antennas with circular symmetry using measured E/H plus co- and cross-polar averaged patterns. This technique can, not only produce a realistic value for ground noise of most small aperture and traveling-wave-type antennas at various orientations but also optimize sensitivity performance of large reflector antennas based just on the feed antenna patterns and dish physical parameters. The analysis confirms the recommended reflector edge illumination guidance but shows that optimum dish parameters for best antenna gain differs from those for best system sensitivity.

1. Introduction

In general, amateur radio astronomers estimate the antenna ground and spillover components of their receiver system noise temperature by subtracting known temperature contributions, such as low noise amplifiers and front-end losses, from calibrations made using the Y-Factor measurement method [5]. This is reasonable providing the calibration can be carried out with sources within the operational situation of interest.

An early approximation was described by Kraus splitting the antenna pattern into 3 regions; the main beam, an orthogonal side-lobe and a back-lobe. Assuming suggested temperatures proposed for these, he arrived at a coarse estimate for the antenna noise temperature [1, p410].

Reference 4 shares an antenna noise calculator based on measured antenna azimuth/elevation patterns and a defined noise temperature environment.

The methods outlined here also rely on antenna polar pattern measurements, assumes these are bore-sight rotationally symmetric and quantizes these sufficient to describe the pattern detail. The analysis is carried out automatically using a spreadsheet and provides a realistic indication of ground noise variation with antenna pointing direction and horizon. The process is also suitable for predicting reflector spillover with only a knowledge of the feed antenna pattern and so is useful for predicting the performance of large dish reflectors.

Section 2 describes the mathematical background theory for the calculations and Section 3 interprets this suggesting a simpler quantized digital approach.

Section 4 demonstrates the analysis technique for ground noise estimation with some examples; the second more detailed example quantifies the variation of ground noise when tilting the antenna towards the horizon.

Section 5 extends the technique to evaluate spillover noise for large dishes using just the feed antenna polar patterns together with the dish physical parameters at the frequency of operation.

The analysis spreadsheets are available via the referenced links and have been encoded and all that is needed is for users to enter their antenna pattern data.

2. Definitions

2.1. *Antenna Noise Temperature*

The antenna noise temperature equation, accounting for both co- and cross-polarization, placed in a non-zero temperature environment is,

$$T_A = \frac{\int_0^{2\pi}\int_{-\pi/2}^{\pi/2}\left[P_C(\theta,\phi)T_{bC}(\theta,\phi)+P_X(\theta,\phi)T_{bX}(\theta,\phi)\right]\sin\theta\, d\theta\, d\phi}{\int_0^{2\pi}\int_{-\pi/2}^{\pi/2}\left[P_C(\theta,\phi)+P_X(\theta,\phi)\right]\sin\theta\, d\theta\, d\phi} \qquad (1)$$

where, θ *and* ϕ, are the azimuth and elevation terms and $P_C(\theta,\phi)$ and $P_X(\theta,\phi)$ are power gain per unit solid angle for co-polar ($_C$) and cross-polar ($_X$) antenna responses respectively.
$\theta = 0$ *and* $\phi = 0$, represents the main beam bore-sight direction.
$T_{bC}(\theta,\phi)$ and $T_{bX}(\theta,\phi)$ represent the corresponding surrounding brightness temperatures per unit solid angle.

This is equation can be implemented in a simpler quantized form as below, by dividing the 4π observation sphere into *M* rotationally symmetric regions to allow a good working estimate of the ground temperature contribution to the telescope system temperature.

$$T_A = \frac{\sum_{m=1}^{M}\left(T_{Cm}G_{Cm}SA_{Cm} + T_{Xm}G_{Xm}SA_{Xm}\right)}{\sum_{m=1}^{M}\left(G_{Cm}SA_{Cm} + G_{Xm}SA_{Xm}\right)} \qquad (2)$$

G_{Cm} and G_{Xm} represent antenna co- and cross-polar pattern power gain levels, assumed constant over *M* solid angles, SA_{Cm} and SA_{Xm} (steradians)

2.2. *Antenna Directivity (Gain)*
Given a spherical set of antenna polar pattern measurements, the antenna directivity, *D*, can be calculated from,

$$D = \frac{4\pi\left[P_C(0,0)+P_X(0,0)\right]}{\int_0^{2\pi}\int_{-\pi/2}^{\pi/2}\left[P_C(\theta,\phi)+P_X(\theta,\phi)\right]\sin\theta\, d\theta\, d\phi} \qquad (3)$$

As before, this equation can be simplified using the quantized integration technique to,

$$D = \frac{4\pi\left(G_{C0}+G_{X0}\right)}{\sum_{n=1}^{N}\left(G_{Cn}SA_{Cn} + G_{Xn}SA_{Xn}\right)} \qquad (4)$$

This directivity figure includes pattern focusing efficiency and will exceed the measured gain by resistive and mismatch losses.

3. Antenna Side-lobe Defining Concept
Ignoring resistive losses and loss due to illumination profile, the maximum gain *G* of an aperture antenna, area *A*, is given by the well-known formula,

$$G = \frac{4\pi A}{\lambda^2} \qquad (5)$$

where λ is the signal wavelength.

For a square aperture side *D*, the aperture area, $A = D^2$.
Now λ/D is a measure of the antenna half power beamwidth = *BW* in radians. So we can re-write the gain equation as,

$$G = \frac{4\pi}{\left(\frac{\lambda}{D}\right)^2} = \frac{4\pi}{BW^2} \qquad (6)$$

Now observe that there are 4π steradians in a sphere and *BW* is approximately the antenna main beam solid angle, also in steradians.

Similarly, for a circular reflector, *G*, becomes,

$$G = \frac{\pi^2 D^2}{\lambda^2} = \frac{4\pi}{\left(\frac{\lambda}{D}\right)^2 \cdot \frac{4}{\pi}} = \frac{4\pi}{BW^2} \qquad (7)$$

So the gain equation is also telling us that the antenna can be considered as producing a number of radial lobes, *G'*, roughly equal to the linear gain figure *G*, over the 4π sphere. One, of course, is the main directional beam and the *G'*-1 remainder can be thought of as much lower level side- and back-lobes equi-spaced over the surface of the sphere; each lobe emanating from the center of the sphere.

This is a useful concept as it gives a measure to the extent of practical side-lobes when determining power radiated or temperature sensed in side-lobes. We can set a level to the *G* - 1 side-lobe beams from antenna power pattern measurements and just sum the side-lobe/equivalent beam contributions over their relevant solid angles using a standard spreadsheet.

3.1. Calculating Side-lobe Temperature Contributions

If the antenna pattern is assumed rotationally symmetric, a particular side-lobe region can be thought of as a number of equivalent side-lobe beams occupying a spherical sector of a sphere as shown in Figure 1.
The solid angles covered by a particular side-lobe level region of Figure 1 are calculated from the spherical sector, solid angle formula,

$$SA_{12} = 4\pi\left[\left(\sin\frac{\phi_2}{2}\right)^2 - \left(\sin\frac{\phi_1}{2}\right)^2\right] = 2\pi\left(\cos\phi_1 - \cos\phi_2\right) \qquad (8)$$

where, ϕ_1 *and* ϕ_2 represent the specified side-lobe sector (elevation) limits.

Dividing the sphere into *M* solid angle sectors, then from each solid angle sector, we can calculate the equivalent number of side-lobe beams within it.

So the number of side-lobe beams in the m^{th} *SA* sector = $\eta_m = \frac{SA_m.G}{4\pi}$ (9)

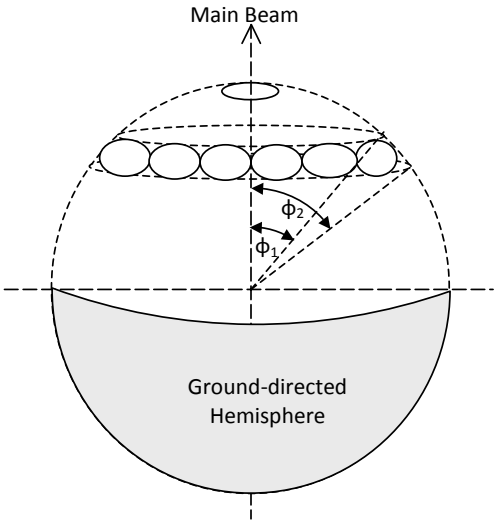

Figure 1 Side-lobe Solid Angle (SA) Spherical Sector Definition, $\phi_2 - \phi_1$

Adapting Equation (2), and assuming the antenna is singly polarized and placed in a closed environment with the walls at ambient temperature, 290°K, the equivalent temperature seen by the m^{th} lobe sector is,

$$T_m = \frac{290.S_m.\eta_m}{\sum_{m=1}^{M} S_m.\eta_m} \quad (10)$$

where, S_m is a nominated side-lobe power gain over the sector SA_m ; the denominator represents the sum of the power levels of all *M* sectors. Setting the enclosed environment allows quantifying the ground temperature seen by ground-pointing antenna lobe/sectors.

4. Examples

The method is first demonstrated with a basic example. In this case, based on an 8 degree beamwidth reflector antenna with published gain 23dB (~x200). The maximum possible gain using the specified beamwidth = 27dB ~ x506.

The overall efficiency then, is 40%, (-4dB gain from maximum = 1/2.5). Efficiency losses of a focus fed parabolic dish include feed losses, illumination profile loss. Directivity losses include spillover and power lost in side-lobes.

4.1 Example 1, Basic Application

The basic example of a co-polar antenna pattern of a parabolic reflector antenna is shown in Figure 2. For the following calculations, it is assumed that this pattern is preserved over the bore-sight axis of revolution.

Here, the pattern is first divided into a number of angular regions by eye, in this case, where the side-lobe levels appear roughly constant, (Column 1, Figure 3). Column 2 represents the mean side-lobe level over each region. Column 3 is the calculated solid angle (Equation 8) whilst Column 4 lists the equivalent number of beams (Equation 9), in this case totaling 506.2, the calculated maximum gain.

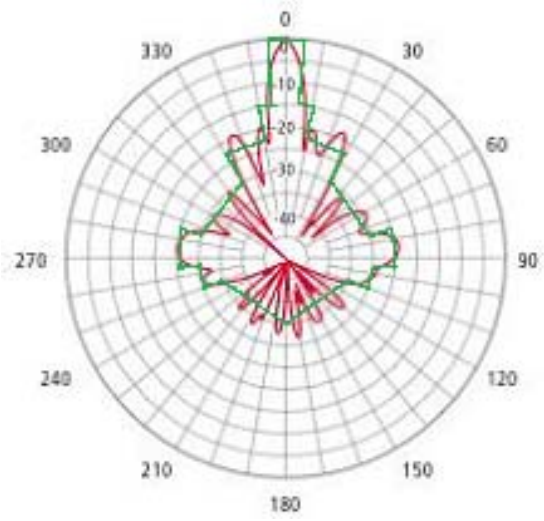

Figure 2 Polar Pattern of Parabolic Dish Example (red), and Approximation (green)

Figure 3 table shows that 49%, (290-148.9)/290, of the power enters through the side-lobes and the antenna pattern efficiency is 51% (=148.9/290) and accounts for 3 dB gain loss from the ideal.
The other 1 dB (ideal gain 27dB, published gain 23dB in the example is reflector illumination loss, feed antenna efficiency etc:

Angle (deg)	SL Level (dB)	Solid Angle (Steradians)	No. Beams	Lobe Sector Temp
0-4	0	0.019	0.8	148.9
4 -10	-15	0.76	3.1	18.5
10-30	-25	0.747	30.1	18.1
30-75	-30	3.817	153.7	29.3
75-95	-25	2.174	87.6	52.8
95-110	-30	1.602	64.5	12.3
110-180	-35	4.133	166.5	10.0
Totals		**12.566**	**506.2**	**290**

Figure 3. Lobe-Sector Temperature Contributions (blue font entries are spreadsheet calculated)

The lobe-sector temperature contributions, Column 5 are calculated using Equation 10.
Figure 3 shows that with the rear hemisphere facing the ground, side/back-lobes (90 to 180 degrees) can contribute 25° or more to a radio telescope system temperature. Also, the side-lobe region 75° - 95° should be kept well clear of horizon/building/tree obstructions.

4.2 Example 2, Estimating System Ground Temperature with Tilted Yagi Antenna
Figure 4 antenna spreadsheet file (Side-lobeTempYagi.xls) applies; measurements in black type (columns F and G) were taken from a professionally designed 22-element Yagi antenna tuned to 595 MHz [6]. The measured co- and cross-polar azimuth patterns are inset with a measured beamwidth of 28.8 degrees.
Data listed in blue type are either pre-set or automatically calculated in the referenced Excel spreadsheet using formulae stored in the spreadsheet file; changing values in columns F and G automatically change the calculated values and results.

A	B	C	D	E	F	G	H	I	J	K	L	M	N	O
BW-Az	BW-El	Max. Gain	Min Angle	Max Angle	Mean level (dB)	Xpol level	SA (sterads)	No: of Beams	CPxT	XPxT	C Power	X Power	C Temp:°K	C+X Temp:°K
28.8	28.8	15.92	0	10	0	-30	0.095	0.30	86.072	0.086	0.297	0.000	81.99	75.25
			10	20	-3	-27	0.284	0.88	128.104	0.510	0.442	0.002	122.02	112.33
		39.1	20	30	-10	-26	0.463	1.44	41.736	1.048	0.144	0.004	39.75	37.37
			30	40	-17	-26	0.628	1.95	11.302	1.423	0.039	0.005	10.77	11.11
			40	50	-21	-27	0.775	2.41	5.547	1.393	0.019	0.005	5.28	6.06
			50	60	-24	-26	0.897	2.79	3.220	2.032	0.011	0.007	3.07	4.59
			60	70	-22	-28	0.993	3.09	5.647	1.418	0.019	0.005	5.38	6.17
			70	80	-27	-25	1.058	3.29	1.903	3.016	0.007	0.010	1.81	4.30
			80	90	-30	-27	1.091	3.39	0.984	1.963	0.003	0.007	0.94	2.57
			90	100	-25	-25	1.091	3.39	3.111	3.111	0.011	0.011	2.96	5.43
			100	110	-23	-27	1.058	3.29	4.780	1.903	0.016	0.007	4.55	5.84
			110	120	-22.0	-25	0.993	3.09	5.646	2.830	0.019	0.010	5.38	7.40
			120	130	-25.0	-27	0.897	2.79	2.557	1.614	0.009	0.006	2.44	3.64
			130	140	-30.0	-25	0.774	2.41	0.698	2.207	0.002	0.008	0.66	2.54
			140	150	-32.0	-27	0.628	1.95	0.357	1.130	0.001	0.004	0.34	1.30
			150	160	-27.0	-25	0.463	1.44	0.832	1.319	0.003	0.005	0.79	1.88
			160	170	-23.0	-27	0.283	0.88	1.279	0.509	0.004	0.002	1.22	1.56
			170	180	-21.0	-30	0.095	0.30	0.681	0.086	0.002	0.000	0.65	0.67
	Totals						12.6	39.1	304.455	27.597	1.050	0.095	290.00	290.00
Notes:	1. Adjust black bold font entries only													
	2. Max linear gain = (180/BW)^2						39.1							
	3. Number of beams in 4pi steradians = linear gain													
	4. Side/backlobe temp: from rear hemisphere (90-180) in Tsys =						30.26	deg K						
	5. Antenna pattern efficiency =						81.3	%						

Figure 4 Side-lobe Spreadsheet Table - Yagi 22-element Example

The method of estimating the system temperature due to ground illumination of the antenna side-lobes is to assume that ground temperature source (assumed here as 290 °K) only occupies the lower hemisphere as seen by the antenna pattern. With this stipulation, when the pointing direction of the antenna is tilted from the vertical new halves of the side-lobe sectors fall within this region whilst on the opposite side, the other half-sectors enter the forward hemisphere. Using this simple algorithm, and summing the lower hemisphere sectors, an estimate of how the ground influences the system temperature with tilting is realized. Figure 5 shows the tilting ground system temperature using the data of Figure 4.

Tilt °K	Tilted Temp:	Incl: Cross Pol:
0	18.99	30.26
10	17.98	28.83
20	16.61	28.06
30	16.61	27.44
40	16.93	27.92
50	19.24	29.68
60	24.45	34.59
70	43.93	52.33
80	104.33	107.71
90	145.00	145.00

Figure 5 System Ground Temperature Variation with Antenna Tilt from Vertical

When tilting the antenna away from the vertical, the proportion of relevant angle ranges directed at ground/warm structures can be estimated and side-lobe sections summed to obtain a new side-lobe temperature result. Pointing an antenna horizontally towards the horizon for example, theoretically, half the antenna pattern hemisphere is now ground-directed, which would result in a ground temperature contribution of 290/2 = 145°K.

Figure 5. Columns 2 and 3 list ground-directed hemisphere noise temperature; column 2, co-polar response only, column 3 including a simulated cross-polar response.

As an example of calculating the values in Figure 5, the result for a 10° tilt using just co-polar data from Figure 5 ('C Temp' column) by examining the tilted sector geometry is,

17.98 = SUM(C Temp: 100° to 180°) + ½.SUM(C Temp: 80° to 100°) (XL1)

Refer to the .xls file in Reference 6 for more detail.

Figure 5 shows that antenna cross-polar performance can have a significant effect on the ground-induced system noise temperature. The cross-polar figures for this antenna show that they need to be much lower than the co-polar side-lobes to minimize their effect. It is interesting to note that the ground system temperature component does not change significantly for tilts up to 50°. This may not be true for sites with positive horizons due to in-leaf trees or buildings: Figure 5 is still relevant in this case and can be used to estimate the increased system noise temperature expanding the range by adapting Equation XL1.

5. Estimating Parabolic Dish Performance

Measurement of large dish antenna patterns requires long antenna ranges, and expensive rotation gear and test equipment. The performance of even very large dishes can however be estimated with well-characterized antenna feed data together with dish physical focus and diameter parameters. With this information, this note describes a method of determining the dish system performance parameters including, optimum *F*/*D* (dish focal length/dish diameter) ratio, beam pattern, gain, efficiency, spillover and *G*/*T* figure ($10.\log_{10}$(antenna gain/system noise)). The previous sections outline the procedure for extracting useful information from the feed antenna patterns. For this example, measurements on a 1420MHz Cantenna antenna are used [7].

5.1. Parabolic Dish Parameters

The profile of the dish is defined by a parabola (see Figure 6) given by,

$$y = \frac{x^2}{4F} \qquad (11)$$

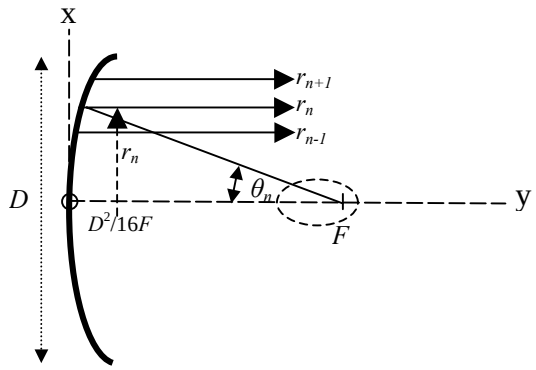

Figure 6. Parabolic Dish + Feed Schematic

Used as an antenna reflector, it has the property that placing a feed antenna at the focal point *F* ensures that all waves generated align in phase at the dish front plane to produce a focused beam with a beamwidth defined by the dish aperture *D* and illumination profile.

The distance from the dish center r_n corresponding to a feed angle offset of θ_n is given by,

$$r_n = 2F\frac{[1-\cos(\theta_n)]}{\sin(\theta_n)}$$

When $r = D/2$, $\tan(\theta) = \dfrac{D/F}{2\left(1-(D/4F)^2\right)}$ (12)

so, given the dish focal distance/dish diameter (F/D) ratio, the feed subtended half-angle θ, at the dish focal distance F can be found.

Maximum gain is achieved if the feed could illuminate the dish with a constant amplitude profile, the beam gain and shape are then defined by,

$$G(\alpha) = \frac{\pi^2 D^2}{\lambda^2}\left[\frac{2J1\left(\frac{\pi}{\lambda}D\alpha\right)}{\left(\frac{\pi}{\lambda}D\alpha\right)}\right]^2 \quad (13)$$

where, D is the dish diameter, α is the beam offset angle in radians, λ is the signal wavelength and $J1$ is the Bessel function of the first kind, first order. Bessel functions are available in most mathematical CAD packages and also conveniently in Excel (using the inbuilt function, BESSELJ()).
Maximum bore-sight gain occurs when $\alpha = 0$.

Generally the feed antenna will not provide a constant illumination over the dish aperture, but will show a more profiled response, preferably rotationally symmetrical. For the purposes of this application, where the feed pattern equivalent temperatures, T_n can be described in spherical sector form, this gain equation can be modified (see Appendix A.1) accordingly to,

$$G(\alpha) = \left(\frac{2\pi}{\lambda}\right)^2\left[r_1\sqrt{T_1}\,j1 + \sum_{n=2}^{N} jn\sqrt{T_n\left(r_n^2 - r_{n-1}^2\right)}\right]^2 / 290 \quad (14)$$

where,

$$j1 = \left[\frac{2J1\left(\frac{2\pi}{\lambda}r_1\alpha\right)}{\frac{2\pi}{\lambda}r_1\alpha}\right] \text{ and, } \quad jn = \left[J0\left(\frac{\pi}{\lambda}(r_n + r_{n-1})\alpha\right)\right]$$

$J0$ is the Bessel function of the first kind, zero order, and is used to approximate the pattern shape contributions of the various annulus rings across the dish aperture, other than the first inner circle, radius r_1.
The annulus illumination amplitudes, T_n apply over the radius range r_n to r_{n-1}, and, n = 1 to N where, $r_N = D/2$.

5.2. Cantenna Feed Data

It is recommended that 360° feed patterns should be taken for E and H planes at 5° intervals, plus intermediate planes if possible, and the results linearly averaged and then partitioned as described above.
To ensure best efficiency estimation, cross-polar patterns should also be available. Together with feed amplitude/temperature pattern measurements.

In practice, it is important to determine the feed aperture phase center (usually just inside the physical aperture) so that it can be accurately placed physically at the dish focal point. The analysis assumes correct alignment.

	A	B	C	D	E	F	G	H	I	J
1	Feed Antenna									
2										
3	theta	Amp	mean LR	SA	G.SA	Tsa	SQRT(Tsa)	Xpol	D	Feed Gain
4								-40	8.21	
5	0	0.00	0	0						8.21
6	5	-0.17	-0.086	0.024	0.023	3.58	1.89			8.12
7	10	-0.32	-0.249	0.072	0.068	10.32	3.21			7.96
8	15	-0.58	-0.448	0.119	0.107	16.35	4.04			7.76
9	20	-0.90	-0.733	0.165	0.139	21.27	4.61			7.47
10	25	-1.37	-1.126	0.210	0.162	24.73	4.97			7.08
11	30	-1.94	-1.643	0.253	0.173	26.49	5.15			6.56
12	35	-2.49	-2.206	0.295	0.177	27.08	5.20			6.00
13	40	-3.16	-2.815	0.334	0.175	26.66	5.16			5.39
14	45	-3.89	-3.510	0.370	0.165	25.22	5.02			4.70
15	50	-4.90	-4.363	0.404	0.148	22.61	4.76			3.84
16	55	-5.88	-5.361	0.435	0.127	19.33	4.40			2.85
17	60	-6.89	-6.356	0.462	0.107	16.35	4.04			1.85
18	65	-8.39	-7.578	0.486	0.085	12.98	3.60			0.63
19	70	-9.81	-9.042	0.507	0.063	9.65	3.11			-0.84
20	75	-11.32	-10.496	0.523	0.047	7.13	2.67			-2.29
21	80	-12.99	-12.075	0.535	0.033	5.08	2.25			-3.87
22	85	-14.63	-13.737	0.54	0.023	3.52	1.88			-5.53
23	90	-16.61	-15.511	0.55	0.015	2.36	1.54			-7.30
24	95	-17.95	-17.229	0.55	0.010	1.59	1.26			-9.02
25	100	-18.79	-18.352	0.54	0.008	1.22	1.11			-10.15
26	105	-19.58	-19.168	0.54	0.007	1.00	1.00			-10.96
27	110	-20.53	-20.028	0.52	0.005	0.80	0.90			-11.82
28	115	-21.27	-20.887	0.51	0.004	0.64	0.80			-12.68
29	120	-21.10	-21.183	0.49	0.004	0.57	0.76			-12.98
30	125	-21.04	-21.070	0.46	0.004	0.56	0.75			-12.86
31	130	-21.09	-21.068	0.43	0.003	0.53	0.73			-12.86
32	135	-21.19	-21.139	0.40	0.003	0.48	0.69			-12.93
33	140	-21.37	-21.277	0.37	0.003	0.43	0.65			-13.07
34	145	-21.90	-21.627	0.33	0.002	0.36	0.60			-13.42
35	150	-23.19	-22.497	0.29	0.002	0.26	0.51			-14.29
36	155	-23.34	-23.264	0.25	0.001	0.19	0.43			-15.06
37	160	-22.24	-22.756	0.21	0.001	0.17	0.42			-14.55
38	165	-21.05	-21.604	0.16	0.001	0.18	0.42			-13.40
39	170	-19.24	-20.051	0.12	0.001	0.18	0.42			-11.84
40	175	-19.30	-19.268	0.07	0.001	0.13	0.36			-11.06
41	180	-19.25	-19.271	0.02	0.000	0.04	0.21			-11.06
42			Col. Sums	12.568	1.899	290.00				

Figure 7. 6" Cantenna Feed Pattern Analysis Spreadsheet

Figure 7 shows a typical feed analysis summary in the spreadsheet *DishCalcsF.xls* [8]. The input data is of an L-band 6 inch diameter, 80 degree beamwidth Cantenna measured at 1420MHz.

The first three columns in the spreadsheet *A*, *B*, *C* list the input data. Column *B* corresponds to the left and right linear averages of the measured pattern plot .

Column C is the sector mid-level,
'Mean' -> 10*LOG((10^(B2/10)+10^(C2/10))/2) (XL2)

Column D is the Sector spherical area from Equation 8
'SA' -> 2*3.142*(COS(A5*3.142/180)-COS(A6*3.142/180)) (XL3)

Column *E*, is the equivalent side-lobe level,
'G.SA' -> =(10^((C6)/10)+10^((H$4)/10))*D6 (XL4)

Column *F,* describes each spherical sector equivalent temperature assumed placed in a 290 K container
'Tsys' -> =290*E6/E42 (XL5)) °

If cross-polar data relative to the co-polar data amplitudes is available for a better directivity and efficiency estimate, then further columns need adding and combined as required by Equation 2. Failing this, in this example a constant cross-polar level of -40dB (column J2) is assumed.

From this data, we can calculate the Directivity = $4\pi/\Sigma(G.SA)$ = 8.21dB and the ground noise temperature assuming the Cantenna is pointed vertically and the lower side-lobe hemisphere is = $\Sigma T_{sal(95\text{-}180)}$ = 9.3°.

Now that the feed antenna is characterized in this way, the forward-looking sector data is suitable for estimating the performance of any feed-reflector dish combination.

5.3. Estimating Parabolic Dish plus Feed Performance.
The parabolic dish focal distance-to-dish diameter ratio *F*/*D* defines the angle subtended by the feed antenna from Equation 12. This angle in turn, defines which feed spherical sectors illuminate which circular ring sections in the dish. Feed antenna spherical sectors that exceed the dish aperture can be used to estimate spillover. The cut-off for ground noise due to spillover is the angle of the dish edge to the horizon angle of 90°, assuming the dish aperture is pointing to the zenith.

5.3. Results.
The analysis spreadsheet *DishCalcsF.xls* uses the Cantenna feed data in the analysis equations of Section 5.1 to synthesize the dish antenna pattern and calculate the various dish parameters as a function of dish focal length to diameter ratio to determine the optimum *F*/*D* ratio.
Figure 8, extracted from the analysis spreadsheet, summarizes the key parameters and performance figures for the feed antenna of Figure 7 when driving a 1.2m dish at 1420 MHz for various *F*/*D* ratios (Row 1). Row 2 lists the corresponding feed-dish subtended angle, chosen to match ranges listed for the feed in Figure 7.

The dish illumination efficiency is calculated by summing the spherical sector temperatures of Figure 7, lying within the feed subtended angle as a ratio of 290 °K. As the focal distance reduces, more of the feed spherical sectors illuminate the dish.

The spillover temperature is calculated by summing the sector temperatures over the range between the *F*/*D* subtended half-angle and 90° - this assumes the dish is directed vertically and ground noise temperature angle is limited by the horizon. The variation of spillover noise with antenna tilting follows the method outlined in Section 4.2.

The feed+dish maximum gain *G*(0), is calculated using Equation 14, setting the Bessel terms, *j0* and *jn* equal to unity; full evaluation is required to calculate the dish antenna polar pattern.
Row 7, estimates the antenna combination radiation efficiency, taking the ratio of dish + feed maximum gain to the aperture maximum gain $= \pi^2 D^2 / \lambda^2$ = 322.3 (for *D* = 1.2m, λ = 0.21m).

F/D	5.73	2.86	1.90	1.42	1.13	0.93	0.79	0.69	0.60	0.54	0.48	0.43	**0.39**	0.36	0.33	0.30	0.27
Subt: Angle(°)	10.0	20.0	30.0	40.0	50.0	60.0	70.0	80.0	90.0	100.0	110.0	120.0	**130.0**	140.0	150.0	160.0	170.0
Illumination Effy.	0.01	0.05	0.10	0.18	0.26	0.35	0.45	0.54	0.63	0.70	0.77	0.83	**0.87**	0.91	0.93	0.95	0.96
Spillover (°K)	277.1	266.8	250.4	229.2	204.4	178.0	150.9	124.2	99.0	76.4	57.1	40.7	**27.7**	18.1	11.0	5.9	2.4
Edge Illumination	0.1	0.2	0.4	0.7	1.1	1.6	2.2	2.8	3.5	4.4	5.4	6.4	**7.6**	9.0	10.5	12.1	13.7
Max Gain	4.0	15.4	33.6	57.2	84.5	113.5	142.7	170.7	196.2	217.4	233.1	243.7	**248.1**	246.2	239.3	228.2	214.0
Radiation Effy.	0.01	0.05	0.10	0.18	0.26	0.35	0.44	0.53	0.61	0.67	0.72	0.76	**0.77**	0.76	0.74	0.71	0.66
G/T+40K	-19.01	-12.98	-9.37	-6.73	-4.61	-2.83	-1.26	0.17	1.50	2.71	3.81	4.80	**5.64**	6.27	6.72	6.97	7.03
G/T+100K	-19.77	-13.76	-10.18	-7.60	-5.57	-3.89	-2.45	-1.18	-0.06	0.91	1.72	2.38	**2.88**	3.19	3.34	3.34	3.20

Figure 8. Feed+Dish Parameter Summary v Dish *F*/*D*

The final two rows offer an indication of the overall system *G*/*T* sensitivity assuming receiver noise temperatures of 40 °K and 100 °K respectively. The Figure 8 tabulated figures also seem to confirm the conventional rule-of-thumb for an optimum feed antenna producing a dish edge illumination of -10dB.

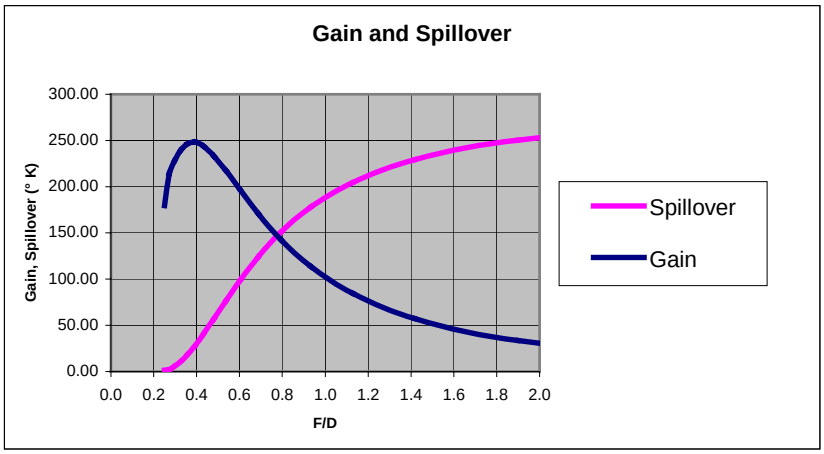

Figure 9. Feed+Dish Gain and Spillover Estimates

Two parameters of primary interest in this tabulated data are plotted in Figure 9. This indicates that for this Cantenna feed, the optimum parabolic dish *F*/*D* ratio producing maximum gain is 0.39. However, in this case the spillover noise temperature appears quite large at 27.7 °K .

The optimum dish *F*/*D* for the chosen feed is tested in Figure 10 using the antenna gain/system noise temperature ratio figure of merit, 10.log(*G*/*T*). To explore this region, Figure 10 also calculates the system *G*/*T* sensitivity for several likely receiver noise temperatures and these show that either a narrower beamwidth feed or a modified dish *F*/*D* ratio down to 0.3 should provide a better system sensitivity result for most practical receiver noise levels. It shows, however, that only the lowest receiver system noise levels benefit significantly from this change.

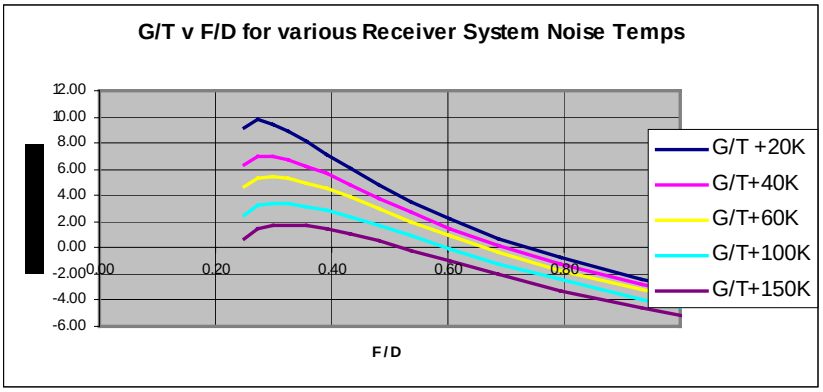

Figure 10. System Sensitivity v F/D Ratio

In Figure 11, the antenna pattern for the feed is plotted together with the predicted dish patterns for *F/D* = 0.39 derived by applying Equation 14. The patterns, are produced using the Excel spreadsheet, *DishCalcsF.xls*, using the spreadsheet sub-panels to calculate the dish ring illuminated contributions and corresponding Bessel terms.

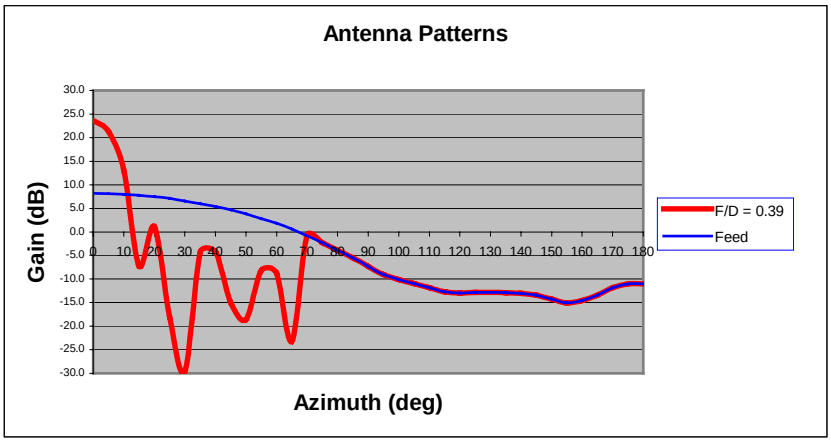

Figure 11. Feed and Predicted Feed+Dish Patterns for *F/D* = 0.39 with 0.8 λ, Feed Blockage

Figure 11 dish pattern at angles greater than 65° should be only taken as a rough guide since the geometrical optics approach adopted ignores diffraction that normally dominates in the rear hemisphere. In practice, diffraction and phasing effects tend to increase side-lobe rippling and complexity and also enhance the 180 degree back-lobe.

Figure 11 is the result of removing the first two center ring terms corresponding to a blockage of 0.164m or 0.8 λ. The effect is to slightly lower the directivity/gain and efficiency, but significantly modify the near side-lobes. Also note that efficiency figures do not include feed match or resistive losses.

6. Spreadsheet Use

The spreadsheets associated with this paper, References 6 and 8, may be used to estimate the performance of custom antennas if suitable antenna pattern data are available. The required computations have been encoded and all that is needed is to enter users pattern data.

Allowed pattern data entries are indicated in black type consistent with the preset angles listed.

7. Conclusions and Discussion

This article describes a simple working spreadsheet method of estimating the effect of side/back-lobes and cross-polar performance on degrading the system noise temperature of a radio telescope over most practical tilting angles and dish geometries. Prediction of large dish antenna performance based on feed antenna radiation pattern measurements is demonstrated including spillover, optimizing *F*/*D* and *G*/*T* plus ratification of the -10dB dish edge illumination popular recommendation. The importance of low antenna cross-polar performance to minimize ground and spillover noise is demonstrated. The spreadsheets are structured to allow entry of custom antenna data for performance prediction of user's antennas.

The method predicts that the optimum parabolic dish antenna *F*/*D* ratio for maximum system sensitivity may not be the same as that for maximum gain due to spillover noise degradation. In the case of this 80 degree beamwidth Cantenna feed example, it appears that the best system sensitivity for sub-50 °K receiver noise temperature systems is possible with a lower dish *F*/*D* ratio of 0.3 rather than 0.4, the value demonstrating maximum gain (see Figure 10). Alternatives here are to reduce the feed beamwidth and corresponding edge illumination or if the situation allows, extend the dish diameter with a suitable reflecting skirt matching the parabola trend. This both reduces the *F*/*D* ratio and increases aperture and gain. Diffraction effects have not been taken into account which tend to increase the back-lobe but these would also reduce with lower edge illumination.

Yagi and helical antenna types have the advantage of size and portability and can be tuned to improve efficiency, so reducing back-lobes at the expense of bandwidth. As basically traveling-wave type antennas, the antenna phase center is near the forward end so that local ground screening is of limited effectiveness. For these antenna types, system sensitivity is best improved by increasing gain and aperture by employing multiple antennas in an array.

8. Acknowledgement

The Yagi and Cantenna Pattern measurement data was provided by, Prof. P.N Wilkinson, School of Physics & Astronomy, University of Manchester.

References

1. Kraus JD. "Radio Astronomy" McGraw-Hill, 1966. p 401.
2. Nikolova N. "Lecture 7: Antenna Noise Temperature and System Signal-to-Noise Ratio", https://www.ece.mcmaster.ca/faculty/nikolova/antenna_dload/current_lectures/L07_Noise.pdf
3. Lambert, K. M., and R. C. Rudduk, ‘‘Calculation and Verification of Antenna Temperature for Earth-Based Reflector Antennas,’’ *Radio Science*, Vol. 27, No. 1, January–February , 1992, pp. 23–30.
4. Galuščák R, Galuščáková P, Mazánek M, Hazdra P, Macáš M. " Antenna Noise Temperature Calculator" http://www.om6aa.eu/Antenna_Noise_Temperature_Calculator.pdf. http://www.om6aa.eu/antc.php
5. Agilent Technologies. "Application Note 57-2, The Y-Factor Method". https://testworld.com/wp-content/uploads/noise-figure-measurement-accuracy-the-y-factor-method.pdf
6. http://www.y1pwe.co.uk/RAProgs/Side-lobeTempYagi.xls
7. Cantenna Calculator, https://www.changpuak.ch/electronics/cantenna.php
8. http://www.y1pwe.co.uk/RAProgs/DishCalcsF.xls
9. Jull, EV. ‘Aperture Antennas and Diffraction Theory’. IET/Peter Peregrinus Ltd, 1981.

PW East V2 September 2024

Appendix 1. Bessel Functions for Circular Aperture Reflector Beam Patterns

For a circular aperture, diameter *D* and a uniform illumination, the antenna beam pattern shape is defined by the first order Bessel function and given by Reference [9],

$$G(\alpha) = \frac{\pi^2 D^2}{\lambda^2}\left[\frac{2J1\left(\frac{\pi}{\lambda}D\alpha\right)}{\left(\frac{\pi}{\lambda}D\alpha\right)}\right]^2 \qquad \text{(A1)}$$

It is convenient in this application to compute the beam shape of the dish with a profiled illumination to split the aperture into a number of ring or annulus sections, assume that the illumination is constant within the ring, and then sum the voltages of these to determine the beam shape.
For any one ring, radius r_1 to r_2, the power is,

$$G_{12}(\alpha) = \frac{4\pi^2}{\lambda^2\left(r_2^2 - r_1^2\right)}\left[\frac{2J1\left(\frac{2\pi}{\lambda}r_2\,\alpha\right)}{\left(\frac{2\pi}{\lambda}r_2\,\alpha\right)}r_2^2 - \frac{2J1\left(\frac{2\pi}{\lambda}r_1\,\alpha\right)}{\left(\frac{2\pi}{\lambda}r_1\,\alpha\right)}r_1^2\right]^2 \qquad \text{(A2)}$$

Since the differential, $\frac{\partial}{\partial x}\left(xJ1(x)\right) = xJ0(x)$

With this identity, Equation (A2) can now be simplified to,

$$G_{12}(\alpha) = \frac{4\pi^2}{\lambda^2}\left(r_2^2 - r_1^2\right)\left[J0\left(\frac{2\pi}{\lambda}\left(\frac{r_1 + r_2}{2}\right)\alpha\right)\right]^2 \qquad \text{(A3)}$$

Extension to *n* rings is based on the summing of ring voltages derived from Equation A3, and this leads to Equation 14 in the main text.

Peter East, *pe@y1pwe.co.uk* is retired from a Defense Electronics career in radar and electronic warfare system design. He has authored a book on Microwave System Design Tools, is a member of the British Astronomical Association since 1975 and joined SARA in 2013. He is active in amateur detection of pulsars using SDRs, and researching low SNR pulsar recognition and analysis. He has recently written two other books, 'Galactic Hydrogen and Pulsars' and 'Small Aperture Pulsar Detection', based on articles written for the BAA RA Group and SARA Journal, describing his work in Radio Astronomy.
He maintains an active RA website at *http://www.y1pwe.co.uk/RAProgs/*